Journal of Materials Science & Technology 32 (2016) 62–67

Contents lists available at ScienceDirect

Journal of Materials Science & Technology

journal homepage: www.jmst.org

Effect of Sodium Metasilicate on Structural, Optical, Dielectric and Mechanical Properties of ADP Crystal

Mohd Anis [1,2], M.D. Shirsat [3], S.S. Hussaini [2], B. Joshi [4], G.G. Muley [1,*]

[1] Department of Physics, Sant Gadge Baba Amravati University, Amravati 444602, Maharashtra, India
[2] Crystal Growth Laboratory, Department of Physics, Milliya Arts, Science and Management Science College, Beed 431122, Maharashtra, India
[3] Intelligent Materials Research Laboratory, Department of Physics, Dr. Babasaheb Ambedkar Marathwada University, Aurangabad 431005, Maharashtra, India
[4] Science and Engineering Research Board, New Delhi 110016, India

ARTICLE INFO

Article history:
Received 8 May 2015
Received in revised form
10 June 2015
Accepted 26 June 2015
Available online 16 September 2015

Key words:
Crystal growth
Nonlinear optical materials
Dielectric properties
Optical properties

For the first time, sodium metasilicate (SMS) doped ammonium dihydrogen phosphate (ADP) crystal was grown by slow evaporation solution technique. The unit cell parameters of grown crystal were determined by means of single crystal X-ray diffraction technique. The qualitative analysis of SMS doped ADP crystal was carried out using energy dispersive X-ray and Fourier transform infrared analysis. The increase in optical transparency of doped ADP crystal was ascertained in the range of 200–900 nm using the UV-visible spectral analysis. The vital optical constants were evaluated using the transmittance data to explore various optical device applications of crystal. The assertive influence of SMS on mechanical and dielectric behavior of ADP crystal was investigated by means of Vickers microhardness analysis and dielectric studies, respectively. The enhancement in second harmonic generation (SHG) efficiency of SMS doped ADP crystal with reference to potassium dihydrogen phosphate (KDP) and ADP was confirmed from Kurtz–Perry SHG test. The Kerr lensing nonlinearity in SMS doped ADP crystal was identified by means of *Z*-scan analysis and the third order nonlinear optical susceptibility (χ^3) was found to be 6.19×10^{-5} esu, which vitalizes its application for laser stabilization systems.

1. Introduction

Ammonium dihydrogen phosphate (ADP) is the potential nonlinear optical (NLO) material exhibiting high nonlinear behavior and good ferroelectric properties which vitalizes its utility for electro-optic modulators, optoelectronics, photonics and large display devices[1,2]. The exceeding use of crystals for various industrial applications has encouraged many researchers to re-investigate the properties of ADP crystal using the different organic and inorganic additives since the past decade. The use of dopants glycine and $_L$-lysine has significantly enhanced the second harmonic generation (SHG) efficiency, UV-visible and electrical properties of ADP crystal[3,4]. It is also evident that the crystalline perfection, optical and electrical properties of ADP crystal can be tuned to large scale using ammonium malate[5]. Influence of carboxylic acids like $_{DL}$-malic acid and oxalic acid on fundamental properties of ADP crystal has been reported[6,7]. The additive ethylene diamine tetraacetic acid (EDTA) has improved the growth period and various properties of ADP crystal[8]. In regime of metallic dopants, a variety of single metallic impurities such as Na, K, Ni and Co have successfully increased the optical, electrical, mechanical, dielectric and thermal properties of ADP crystal[9–13]. This declares the highly favorable impetus of metallic dopants for ADP crystal. However, until this date effect of bimetallic impurities on different properties of ADP crystal has not been explored. With the aim to achieve the high quality ADP crystal for applications of laser assisted technological devices a bimetallic impurity such as sodium metasilicate (SMS) has been firstly doped in ADP crystal. In this study pure and SMS doped ADP crystals have been comparatively investigated by structural, UV-visible, SHG, *Z*-scan, microhardness and dielectric studies with focus centered to explore the effective utility of grown crystal for laser applications.

2. Experimental

The high purity ADP salt was dissolved in deionized water to obtain the supersaturated solution of ADP at room temperature. To grow the cost effective and commercial crystal the measured quantity of 0.1 mol% of SMS (Na_2SiO_3) was gradually added to the

* Corresponding author. Ph.D.; Tel.: +91 9850325379; Fax: +917212660949/2662135.
E-mail address: gajananggm@yahoo.co.in (G.G. Muley).

http://dx.doi.org/10.1016/j.jmst.2015.09.010

Fig. 1. Photograph of SMS-ADP crystals.

supersaturated solution of ADP with continuous and uniform speed of stirring. The solution was allowed to agitate for 6 h to assure the homogeneous doping throughout the supersaturated solution of ADP. The SMS doped ADP solution was filtered and kept for isothermal slow solution evaporation in a constant temperature bath of accuracy ±0.01 °C. The optically transparent SMS doped ADP (SMS-ADP) crystals harvested within 13–15 days are shown in Fig. 1.

3. Results and Discussion

3.1. Single crystal X-ray diffraction

The crystals were subjected to single crystal X-ray diffraction (XRD) analysis using the Enraf Nonius CAD-4 crystal X-ray diffractometer. The pure and SMS doped ADP crystals were confirmed to have the tetragonal crystal structure and the slight changes were identified in the unit cell parameters of SMS-ADP crystal. The XRD data are discussed in Table 1 and the increase in volume of SMS-ADP crystal might have been attributed to the successful incorporation of SMS in lattice sites of ADP crystal.

3.2. Elemental analysis

The incorporation of SMS in ADP has been qualitatively confirmed by means of energy dispersive spectroscopic (EDS) technique using the HITACHI S4700 instrument. The grown SMS-ADP crystals were powdered and subjected to EDS analysis (energy range = 0 to 10 keV). The recorded EDS spectrum of SMS-ADP crystal is shown in Fig. 2(a). The peaks observed at 1 and 1.78 keV evidence the presence of sodium (Na) and silicon (Si) ions in the crystal lattice of ADP.

Table 1
Crystallographic data

Crystal	Crystal system	Cell parameters (nm)	Volume (nm^3)	Space group
ADP	Tetragonal	$a = b = 0.751$, $c = 0.756$	0.426	*I*-42*d*
SMS-ADP	Tetragonal	$a = b = 0.752$, $c = 0.761$	0.430	*I*-42*d*

3.3. Fourier transform infrared analysis

The functional groups of grown crystal were identified by means of Fourier transform infrared (FT-IR) analysis using Bruker attenuated total reflection (ATR) spectrometer. The recorded FT-IR spectrum of SMS doped ADP crystal is shown in Fig. 2(b). The absorption peaks cited at wavenumber 3790 and 3232 cm^{-1} correspond to Si—O—H stretching vibrations. The P—H stretching vibration is observed at 2362 cm^{-1}. The characteristic NO_2 asymmetric vibration is attributed at 1587 cm^{-1}. The sharp peak of N—H stretching vibrations occurs at 1417 cm^{-1}. The P═O stretching vibration is observed at 1253 cm^{-1}. The absorption peak at 1052 cm^{-1} corresponds to the Si—O—Si asymmetric stretching vibrations. The NO_2 bending mode of vibration is attributed at 680 cm^{-1}.

3.4. Optical studies

3.4.1. UV-visible spectral analysis

The crystals with high optical homogeneity can be readily used for applications in wide range of optical devices. The UV-visible transmittance spectrum of pure and SMS doped ADP crystal was recorded in the range of 200–900 nm using the Shimadzu UV-2450 spectrophotometer. The analysis of spectrum (Fig. 3(a)) in visible region reveals that the transparency of ADP and SMS-ADP crystals is up to 79% and 86%, respectively. The enhanced transparency of SMS-ADP crystal by 7% justifies the assertive role of dopant in minimizing the defect centers and solvent inclusions which attributed the reduced optical scattering within the crystal system[14]. The high optical transparency window of SMS-ADP crystal is of huge advantage for UV-tunable lasers, NLO and frequency conversion devices[15]. The dependence of absorption coefficient (α) on incident photon

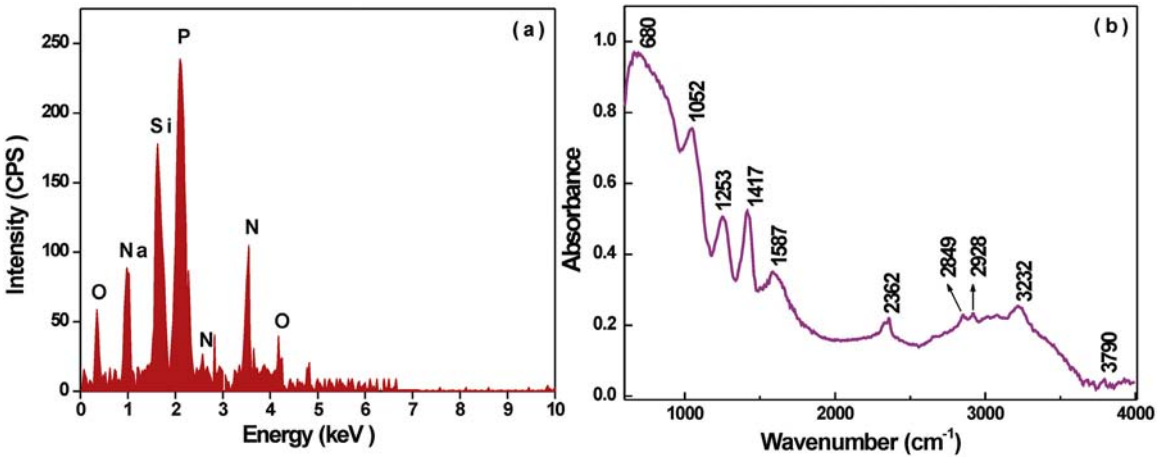

Fig. 2. (a) EDX spectrum of SMS-ADP, (b) FT-IR spectrum of SMS-ADP crystal.

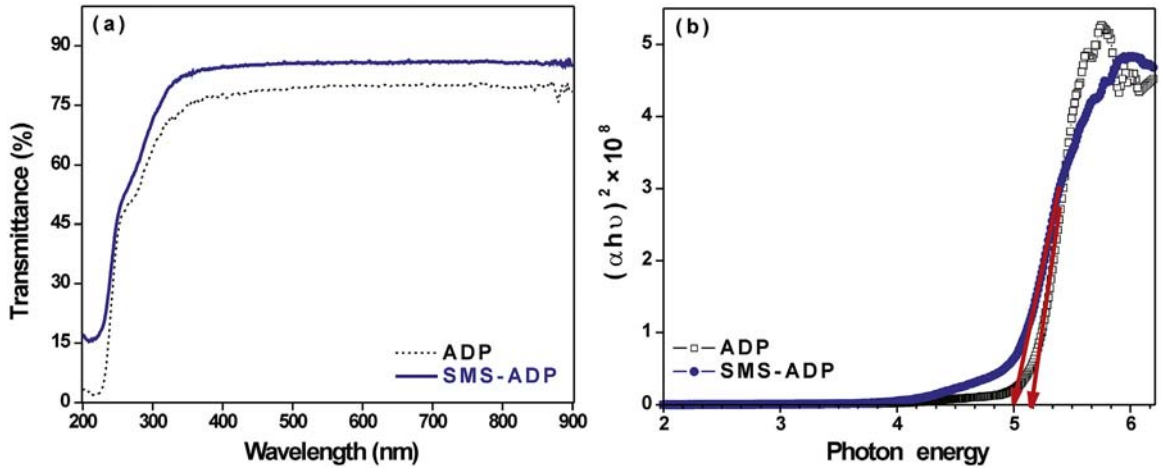

Fig. 3. (a) UV-vVisible transmittance spectrum, (b) Tauc's plot.

energy ($h\nu$) is related as $(\alpha h\nu)^2 = A(h\nu - E_g)$, where E_g is the energy band gap of the material. The E_g of grown crystal has been determined from the Tauc's extrapolation plot shown in Fig. 3(b). In the present study, the E_g of ADP and SMS-ADP crystal is found to be 5.1 and 5 eV, respectively, which is wide enough to exploit the SMS-ADP crystal for optoelectronics device applications[15]. The optical density of the material medium can be understood from the nature of refractive index ($n = 1/T + (1/T - 1)$, where T is the transmittance of the material), as shown in Fig. 4(a)[16]. The SMS-ADP crystal possesses lower refractive index than ADP in visible region which makes it a more suitable material for calibrating the figure of merit of reflectors, resonators and filters which are vital optical components in large laser systems[17]. The reflectance (R) offered by crystals in visible region is shown in Fig. 4(b). The electromagnetic energy is lost within material medium while propagation can be analyzed by observing the behavior of extinction coefficient ($K = \alpha\lambda/4\pi$), as shown in Fig. 5. The high percent of transparency, lower refractive index, lower reflectance and extinction coefficient suggest the potential candidature of SMS-ADP crystal as antireflecting material demanded for coating solar thermal devices[15,18].

3.4.2. Kurtz–Perry powder SHG test

In order to confirm the NLO behavior, the crystal samples were powdered and subjected to SHG efficiency test using the Kurtz–Perry powder technique. The Q-switched Nd:YAG laser beam ($\lambda = 1064$ nm, 6 ns, 10 Hz, 5.4 μJ/pulse) was made normally incident on the powdered sample of KDP, ADP and SMS-ADP crystals. The emergence of intense green signal confirmed the NLO behavior of each sample and the output SHG intensity of each sample is shown in Fig. 6. The SHG efficiency of SMS-ADP crystal is found to be 2.26 times that of KDP and 1.25 times that of ADP crystal material. The enhancement in SHG efficiency might have been observed due to the modified molecular orientation of ADP crystal due to the incorporation of ionic impurities of SMS. The SHG efficiency of SMS-ADP crystal is found as superior to oxalic acid[7], potassium chloride[10] and cobalt ion[13] doped ADP crystals. The high SHG efficiency strongly advocates the prominence of SMS-ADP crystal for laser frequency conversion devices.

3.4.3. Z-scan analysis

The Z-scan is the most efficient and vital technique developed by Bahae et al. to explore the third order nonlinear behavior of the material at desired laser wavelength[19]. In the present Z-scan setup (Table 2) the polarized beam of He–Ne laser is tightly focused on SMS-ADP crystal (1 mm) through a converging lens and the crystal was moved to and fro about the beam irradiated path focus ($Z = 0$). In closed aperture Z-scan configuration the position of crystal sample was changed along the Z direction and the transmittance was recorded through the closed slit of photo detector placed at far field. The close aperture Z-scan curve (Fig. 7(a)) of SMS-ADP crystal shows

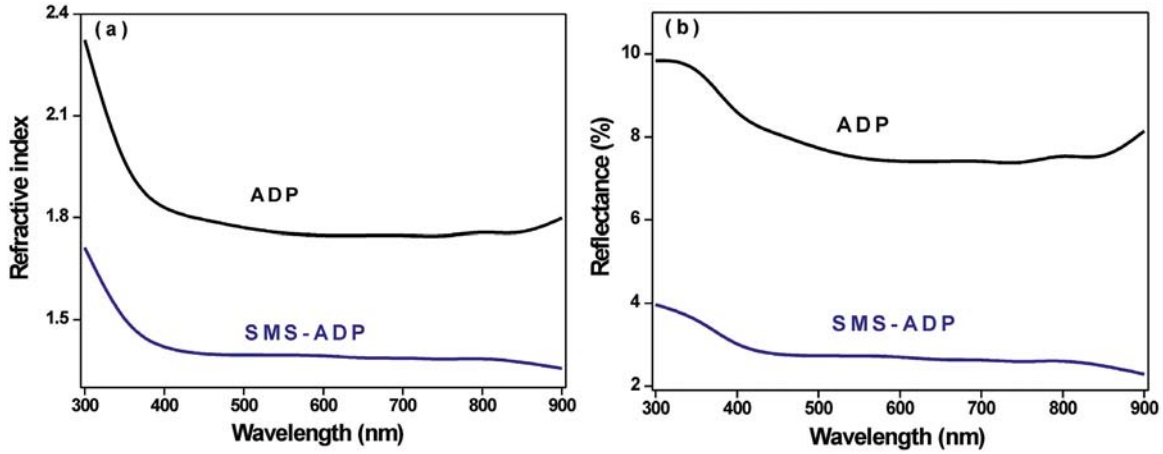

Fig. 4. Plot of (a) refractive index and (b) reflectance as a function of wavelength.

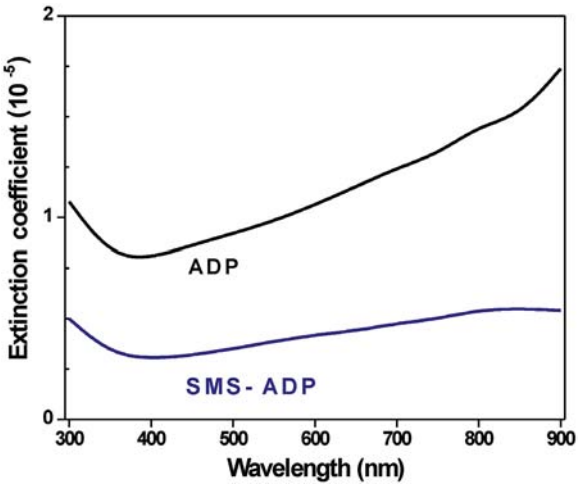

Fig. 5. Plot of extinction coefficient as a function of wavelength.

the valley to peak phase shift which confirms the self focusing effect resulting to positive NLR response[20]. The high magnitude of positive NLR (n_2) identifies the promising Kerr lens mode locking (KLM)[21] potential of SMS-ADP crystal. The relation between axis phase shift ($\Delta\Phi$) and peak to valley transmittance difference (ΔT_{p-v}) is given as[19],

$$\Delta T_{p-v} = 0.406(1-S)^{0.25}|\Delta\phi| \quad (1)$$

where $S = 1 - \exp(-2r_a^2/\omega_a^2)$ is the aperture linear transmittance, r_a is the aperture radius and ω_a is the beam radius at the aperture.

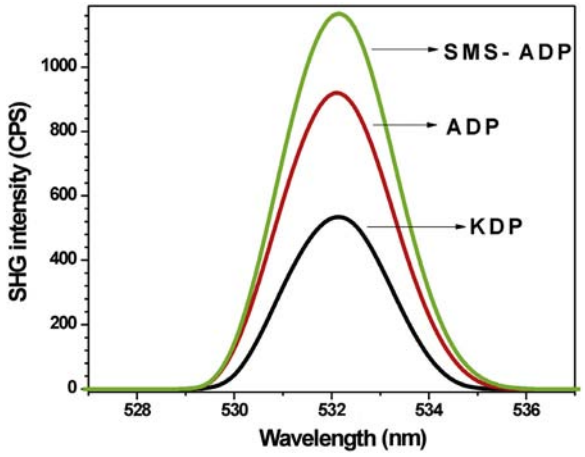

Fig. 6. Plot of SHG output intensity.

Table 2
Z-scan analysis data

Parameters	Magnitude
Laser wavelength (λ)	632.8 nm
Laser power (P)	10 mW
Lens focal length (f)	20 cm
Optical path distance (Z)	113 cm
Beam waist radius (ω_a)	1 mm
Aperture radius (r_a)	15 mm
Incident intensity at the focus (I_o)	2.3375 kW/m^2
Nonlinear refraction (n_2)	5.94×10^{-10} cm^2/W
Nonlinear absorption (β)	2.81×10^{-5} cm/W
Cubic susceptibility (χ^3)	6.19×10^{-5} esu

The magnitude of nonlinear refractive index (n_2) is calculated using the relation[19],

$$n_2 = \frac{\Delta\phi}{KI_0L_{eff}} \quad (2)$$

where $K = 2\pi/\lambda$ (λ is the laser wavelength), I_0 is the intensity of the laser beam at the focus ($Z = 0$), $L_{eff} = (1 - \exp(-\alpha L))/\alpha$ which is the effective thickness of the sample depending on linear absorption coefficient (α) and the thickness of the sample (L). The magnitude of n_2 of SMS-ADP crystal is found to be 5.94×10^{-10} cm^2/W which is notably higher than potential technological crystals used in laser systems[22]. The open aperture *Z*-scan curve (Fig. 7(b)) of SMS-ADP crystal reveals the saturable absorption (SA) phenomenon which is attributed to higher ground state linear absorption over the excited state absorption[23]. The nonlinear absorption coefficient (β) value of crystal has been calculated from following equation[19],

$$\beta = \frac{2\sqrt{2}\Delta T}{I_0L_{eff}} \quad (3)$$

where ΔT is the one valley value at the open aperture *Z*-scan curve. The β of SMS-ADP crystal is found to be 2.81×10^{-5} cm/W. The cubic susceptibility (χ^3) defines the polarizing ability of the material which can be calculated using the following equations[19],

$$\mathrm{Re}\,\chi^{(3)}(\mathrm{esu}) = 10^{-4}\left(\varepsilon_0C^2n_0^2n_2\right)/\pi\left(\mathrm{cm}^2/\mathrm{W}\right) \quad (4)$$

$$\mathrm{Im}\,\chi^{(3)}(\mathrm{esu}) = 10^{-2}\left(\varepsilon_0C^2n_0^2\lambda\beta\right)/4\pi^2\left(\mathrm{cm}/\mathrm{W}\right) \quad (5)$$

$$\chi^3 = \sqrt{\left(\mathrm{Re}\,\chi^3\right)^2 + \left(\mathrm{Im}\,\chi^3\right)^2} \quad (6)$$

where ε_0 is the vacuum permittivity, n_0 is the linear refractive index of the sample and c is the velocity of light in vacuum. The larger χ^3 of crystal system confirms the high polarizing nature of SMS-ADP crystal and it is found to be 6.19×10^{-5} esu. The larger value of χ^3 indicates the enhanced photoinduced intermolecular charge transfer through π-electron conjugate system[24]. The SMS-ADP crystal with higher χ^3 could be a better replacement of several doped ADP crystals[4,25,26].

3.5. Microhardness studies

The Vicker's microhardness studies were performed to unfold the influence of SMS on crystal strength and lattice perfection of ADP crystal. To study the hardness behavior, different loads (25 to 100 g) were applied for the period of 10 s on <001> face of ADP and SMS-ADP crystal and the corresponding diagonal length was measured. The nearly square shaped indentations were observed on the indented surface which indicates the presence of uniform interatomic bonding and spacing in SMS-ADP crystal. The hardness number (H_v) of the crystals was calculated using relation $H_v = 1.8544\times P/d^2$, where P is the applied load in kg and d is the diagonal length in mm[27]. The variation of hardness number with increasing load is shown in Fig. 8(a). It reveals that the hardness of SMS-ADP crystal is superior to ADP crystal. The work hardening index n was derived using the Meyer's equation given as: $\log P = \log K_1 + n\log d$. The plot between $\log d$ and $\log P$ is shown in Fig. 8(b). The slope of the line gives the value of n. The SMS-ADP crystal with large value of n (3.2) belongs to the category of soft materials satisfying the Onitsch results[28]. The hardness dependent yield strength ($\sigma_y = (0.1)^{n-2}H_v/3$) and elastic stiffness ($C_{11} = H_v{}^{7/4}$) of crystals has also been evaluated at same loads. The higher magnitude of elastic stiffness of SMS-ADP crystal confirmed the strong interatomic bonding forces between the adjacent atoms[29]. The

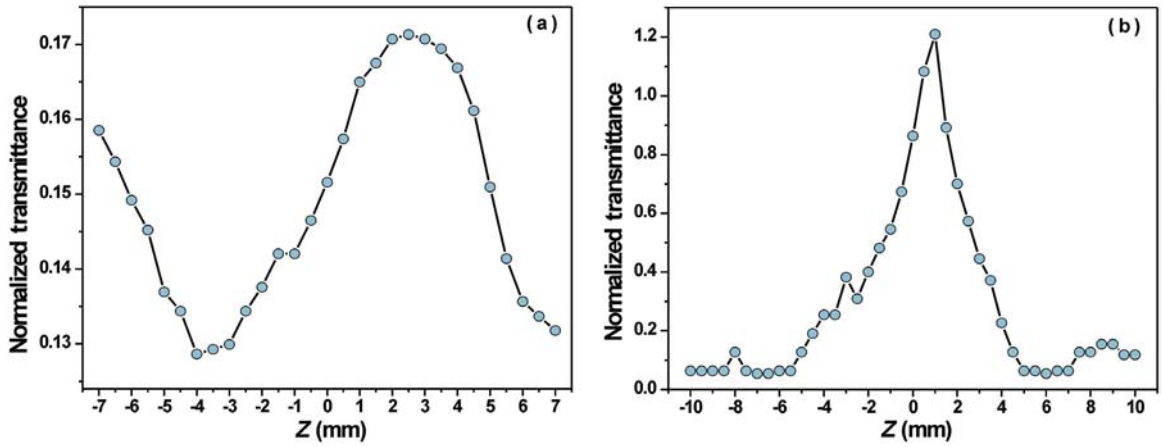

Fig. 7. (a) Close and (b) open aperture *Z*-scan transmittance curves.

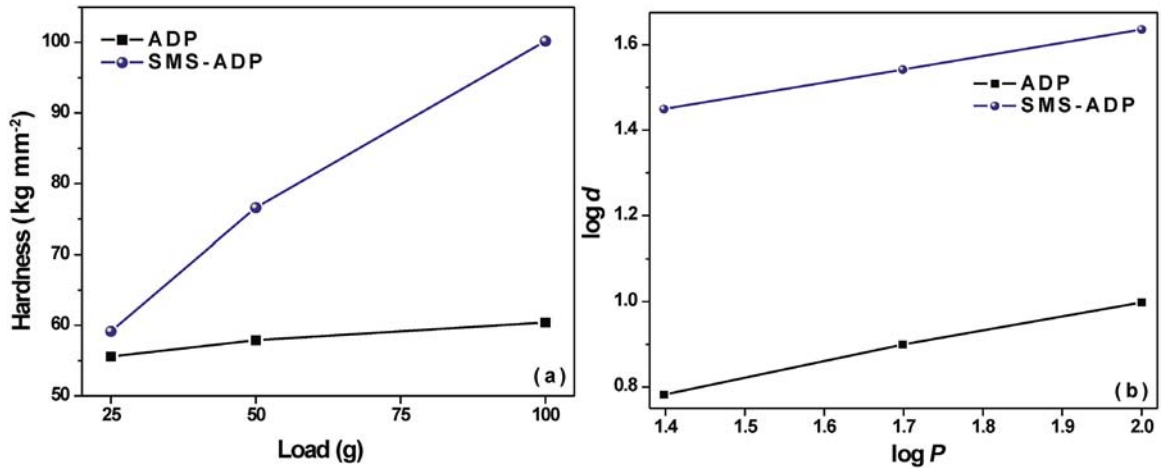

Fig. 8. (a) Load dependent hardness, (b) plot of log*d* vs log*P*.

hardness data of pure and doped ADP crystal are discussed in Table 3. The SMS-ADP crystal exhibits high hardness number, high yield strength and high elastic stiffness which are of huge importance while tuning and processing the material for fabricating NLO devices.

3.6. Dielectric studies

The dielectric properties of the grown crystal have been evaluated in the range of 30 to 120 °C at a frequency of 100 kHz using the HIOKI-3532 LCR cubemeter. Before the analysis the crystal surfaces were smoothly applied with the silver paste so as to attain good electrical contact and measure the data with high accuracy. The dielectric constant of the materials is attributed to active electronic, ionic, space charge and dipolar polarization mechanisms[30]. The dependence of dielectric constant ($\varepsilon_r = Cd/\varepsilon_0 A$) on temperature is depicted in Fig. 9(a). It is observed that the dielectric constant of the crystals increases with increasing temperature. It is contributed to the high space charge polarization of molecular dipoles in high temperature range[31]. The lower dielectric constant of SMS-ADP crystal confirms the low electrical power consumption capability which is a vital parameter for designing photonics, microelectronics[32], broad band electro-optic modulators (EOM)[33], field detectors and THz wave generators[34]. According to Miller's law, the lower dielectric constant facilitates the enhancement in SHG coefficient of the crystal[28], which is also observed in the case of SMS-ADP crystal. The profile of dielectric loss (Fig. 9(b)) of material assists to evaluate the extent of loss of electrical energy in the form of heat in material medium. It is observed that the dielectric loss of SMS-ADP crystal is lower than ADP throughout the temperature range. The lower dielectric loss of SMS-ADP crystal defines the superior optical quality and less concentration of electrically active defects which is vital parameter for NLO applications[35].

Table 3
Microhardness parameters along <001> face

Crystal	H_v (kg/mm^2)	n	σ_y (MPa)	C_{11} (GPa)
ADP	57.96	2.8	11.94	20.91×10^6
SMS-ADP	78.65	3.2	16.21	36.72×10^6

4. Conclusion

Good quality SMS-ADP crystals were successfully grown by slow solution evaporation technique. The single crystal XRD confirmed the unit cell parameters and tetragonal structure of pure and SMS doped ADP crystals. The EDS analysis confirmed the incorporation of SMS in ADP and the functional groups of grown crystal were identified using the FT-IR analysis. The UV-visible studies revealed that the SMS-ADP crystal offered the enhanced optical transparency of

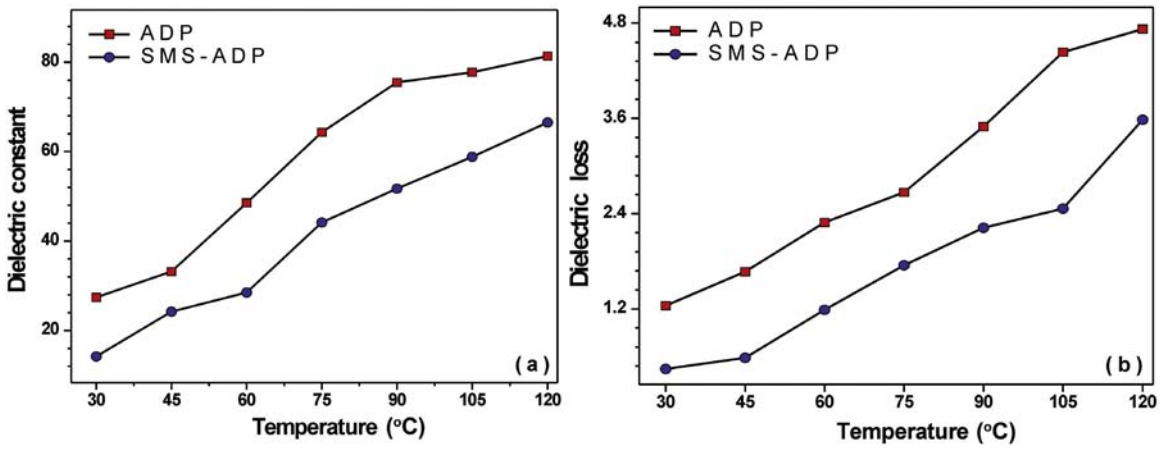

Fig. 9. Temperature dependent (a) dielectric constant and (b) dielectric loss.

86%, band gap of 5 eV and superior optical parameters than ADP crystal which vitalized its use for optical device applications. The microhardness studies revealed that SMS had largely enhanced the hardness, yield strength and elastic stiffness of ADP crystal. The determined low dielectric nature of SMS-ADP crystal was advantageous for fabrication of microelectronics and EOM devices. The SHG efficiency of SMS-ADP crystal was 2.26 times that of KDP and 1.25 times that of ADP crystal. The *Z*-scan analysis confirmed the positive NLR phase transition and its magnitude was found to be 5.94×10^{-10} cm^2/W. SMS-ADP crystal was promising Kerr lens mode locking material. The enhanced cubic nonlinearity of SMS-ADP crystal was of order 10^{-5} esu which confirmed the sustained mobility of intermolecular charge transfer due to modified molecular orientation of SMS-ADP crystal. All of the above studies infered that SMS-ADP crystal could be a potential material for distinct laser assisted applications.

References

[1] T.C. Upadhyay, D. Joshi, Ind. J. Pure Appl. Phys. 50 (2012) 167–174.
[2] S. Ji, F. Wang, L. Zhu, X. Xu, Z. Wang, X. Sun, Sci. Rep. 3 (2013) 1605, doi:10.1038/srep01605.
[3] R.N. Shaikh, M. Anis, A.B. Gambhire, M.D. Shirsat, S.S. Hussaini, Mat. Res. Express 1 (2014) 015016, doi:10.1088/2053-1591/1/1/015016.
[4] R.N. Shaikh, M. Anis, M.D. Shirsat, S.S. Hussaini, IOSR-JAP 6 (2014) 42–46.
[5] P. Rajesh, P. Ramasamy, G. Bhagavannarayana, J. Cryst. Growth 311 (2009) 4069–4075.
[6] P. Rajesh, P. Ramasamy, J. Cryst. Growth 311 (2009) 3491–3497.
[7] P. Rajesh, P. Ramasamy, Physica B 404 (2009) 1611–1616.
[8] A. Rahman, J. Podder, Ind. J. Pure Appl. Phys. 86 (2012) 15–21.
[9] N. Joseph John, C.K. Mahadevan, Mater. Manuf. Process. 23 (2008) 809–815.
[10] S. Meenakshisundaram, S. Parthiban, G. Madhurambal, S.C. Mojumdar, J. Therm. Anal. Calorim. 96 (2009) 77–80.
[11] P. Rajesh, P. Ramasamy, Mater. Lett. 63 (2009) 2260–2262.
[12] P. Rajesh, P. Ramasamy, C.K. Mahadevan, Mater. Lett. 64 (2010) 1140–1143.
[13] P. Rajesh, P. Ramasamy, B. Kumar, G. Bhagavannarayana, Physica B 405 (2010) 2401–2406.
[14] M. Senthil Pandian, N. Pattanaboonmee, P. Ramasamy, P. Manyum, J. Cryst. Growth 314 (2011) 207–212.
[15] M. Anis, M.D. Shirsat, G. Muley, S.S. Hussaini, Physica B 449 (2014) 61–66.
[16] N.A. Bakr, A.M. Funde, V.S. Waman, M.M. Kamble, R.R. Hawaldar, D.P. Amalnerkar, S.W. Gosavi, S.R. Jadkar, Pramana-J. Phys. 76 (2011) 519–531.
[17] E.F. Schubert, J.K. Kim, J.Q. Xi, Phys. Stat. Sol. B 244 (2007) 3002–3008.
[18] T.C. Sabari Girisun, S. Dhanuskodi, Cryst. Res. Technol. 44 (2009) 1297–1302.
[19] M.S. Bahae, A.A. Said, T.H. Wei, D.J. Hagan, E.W. Van Stryland, IEEE J. Quantum Electron 26 (1990) 760–769.
[20] X.Q. Wang, Q. Ren, J. Sun, H.L. Yang, T.B. Li, H.L. Fan, G.H. Zhang, D. Xu, J.H. Zhao, Cryst. Res. Technol. 44 (2009) 657–668.
[21] L.T. Jin, X.Q. Wang, Q. Ren, N.N. Cai, J.W. Chen, T.B. Li, X.T. Liu, L.N. Wang, G.H. Zhang, L.Y. Zhu, D. Xu, J. Cryst. Growth 356 (2012) 10–16.
[22] A. Major, J.S. Aitchison, P.W.E. Smith, F. Druon, P. Georges, B. Viana, G.P. Aka, Appl. Phys. B 80 (2005) 199–201.
[23] X.Q. Wang, Q. Ren, H.L. Fan, J.W. Chen, Z.H. Sun, T.B. Li, X.T. Liu, G.H. Zhang, D. Xu, W.L. Liu, J. Cryst. Growth 312 (2010) 2206–2214.
[24] V. Singh, P. Aghamkar, R.K. Malik, Appl. Phys. B 115 (2013) 391–395.
[25] R.N. Shaikh, M. Anis, M.D. Shirsat, S.S. Hussaini, Spectrochim Acta A 136 (2015) 1243–1248.
[26] R.N. Shaikh, M.D. Shirsat, P.M. Koinkar, S.S. Hussaini, Opt. Laser Technol. 69 (2015) 8–12.
[27] R. Robert, C. Justin Raj, S. Krishnan, R. Uthrakumar, S. Dinakaran, S. Jerome Das, Physica B 405 (2010) 3248–3252.
[28] M. Senthil Pandian, P. Ramasamy, J. Cryst. Growth 312 (2010) 413–419.
[29] G. Pabitha, R. Dhanasekaran, Mater. Sci. Eng. B 177 (2012) 1149–1155.
[30] M. Anis, R.N. Shaikh, M.D. Shirsat, S.S. Hussaini, Opt. Laser Technol. 60 (2014) 124–129.
[31] S.R. Thilagavathy, K. Ambujam, Trans. Ind. Inst. Met. 64 (2011) 143–147.
[32] M. Anis, G.G. Muley, G. Rabbani, M.D. Shirsat, S.S. Hussaini, Mater. Technol. Adv. Perform. Mater. 30 (2015) 129–133.
[33] N.N. Shejwal, M. Anis, S.S. Hussaini, M.D. Shirsat, Phys. Scr. 89 (2014) 12807–128011.
[34] G. Shanmugam, K. Thirupugalmani, R. Rakhikrishna, J. Philip, S. Brahadeeswaran, J. Therm. Anal. Calorim. 114 (2013) 1245–1254.
[35] V. Kannan, K. Thirupugalmani, G. Shanmugam, S. Brahadeeswaran, J. Therm. Anal. Calorim. 115 (2014) 731–742.